Scientia Iranica B (2015) 22(6), 2163–2169

SCIENTIA IRANICA

Sharif University of Technology
Scientia Iranica
Transactions B: Mechanical Engineering
www.scientiairanica.com

Mitigation of cogging torque for brushless interior permanent-magnet motors

Y.-C. Wu* and Y.-T. Chen

Department of Mechanical Engineering, National Yunlin University of Science & Technology, Douliou, Yunlin, Taiwan 640, R.O.C.

Received 22 May 2014; received in revised form 24 February 2015; accepted 22 August 2015

KEYWORDS
Cogging torque; Brushless Interior Permanent-Magnet (IPM) motor; Exterior-rotor type; Finite-element analysis.

Abstract. In brushless Interior Permanent-Magnet (IPM) motors there exists an oscillatory torque that is induced by the mutual interaction of permanent magnets mounted on the rotor and a slotted structure formed on the stator, generally called the cogging torque. This undesirable torque mainly causes vibration, position inaccuracy and acoustic noise from brushless IPM motors. This paper investigates the influence of geometric parameters on the cogging torque of brushless IPM motors. An exterior-rotor brushless IPM motor, with embedded magnet poles in a V-shape, is introduced. With the aid of commercial finite-element analysis software, cogging torque waveforms of brushless IPM motors are accurately calculated. The effects of geometric parameters on the cogging torque, including magnet span angle of the rotor, shoe depth and shoe ramp of the stator, dummy slots notched on the stator, depth of the dummy slot and dummy slots notched on both the stator and rotor, are discussed. Ten design cases, with different values of design parameter, are presented to effectively mitigate the cogging torque. Design case X of the brushless IPM motor, with dummy slots on the stator, performs better than the original brushless IPM motor, with a 79.1% decrease in the peak value of the cogging torque.

1. Introduction

An electric motor is a kind of electric machine that converts electrical energy via magnetic energy into mechanical energy. It is widely used in various domestic and industrial applications. Statistically, the number of brushless permanent-magnet (BLPM) motors being used has increased rapidly in recent years [1]. The BLPM motor is inherently maintenance free because of the absence of mechanical commutators. The BLPM motor also possesses high efficiency due to the absence of field coil loss. Generally, BLPM motors can be classified in two major categories. The first category is a motor with permanent magnets mounted on the inner or outer surface of the rotor, which is usually called a brushless Surface-mounted Permanent-Magnet (SPM) motor. The second category is a motor with permanent magnets placed in the interior of the rotor core, which is commonly called a brushless Interior Permanent-Magnet (IPM) motor. In addition to the electromagnetic torque, the IPM motor also generates the reluctance torque, due to the rotor variable magnetic reluctance, i.e. the rotor saliency. Therefore, brushless IPM motors possess greater output torque, higher power density and better permanent magnetic material utilization than brushless SPM motors [2]. With the inherent advantages of a long constant power operating range and a magnet-retaining design to prevent magnets from flying apart, the brushless IPM motor provides a good solution for vehicle propulsion applications and variable speed operations. However, inherently, within the BLPM motor, there exists a cogging torque, which is an undesirable component for the operation of such a motor. The cogging torque is an

*. *Corresponding author. Tel.: 886(5)534-2601 ext. 4125; Fax: 886(5)531-2062*
E-mail address: wuyc@yuntech.edu.tw (Y.-C. Wu)

open circuit and oscillatory torque that causes a torque ripple, as well as preventing a smooth rotation of the BLPM motor. It may also induce mechanical vibration, speed ripples, acoustic noise, possible resonance and position inaccuracy, particularly in light-load and low-speed applications [3-5]. For permanent-magnet motor designers, mitigation of the cogging torque is a major concern, especially in the preliminary design stage. Technically, several approaches have been developed and employed to minimize the cogging torque by modifying the rotor and stator configurations of BLPM motors. These techniques include designing the shape and dimension of air-barriers [5], determining the number of slots/pole combinations [6], discrete or step skewing of permanent-magnet blocks on the rotor [3,7-9], optimizing the polar arc of the permanent magnet [9], adding auxiliary teeth and slots on the stator [7,10], skewing the lamination stack of the stator [11], alternating slot openings of the stator [12], integrating a mechanical gear with the stator to generate tooth space on pole shoes [13,14], etc. However, the feasibility of reducing cogging torques for brushless IPM motors with buried permanent magnet poles in a V-shape by applying the foregoing approaches is not mentioned in these studies.

This paper investigates the influence of geometric design parameters on the cogging torque of a brushless IPM motor. The structural configuration of a brushless IPM motor with an exterior rotor containing embedded magnet poles, with magnets in a V-shape, is first introduced. The effects of geometric parameters on the cogging torque, including the magnet span angle of the rotor, the shoe depth and shoe ramp of the stator, dummy slots notched on the stator, the depth of the dummy slot and dummy slots notched on both the stator and rotor, are then discussed. A 2-D Finite-Element Analysis (FEA) package is applied to assist in accurately evaluating the peak value of the cogging torque, in order to obtain a brushless IPM motor with low cogging torque.

2. An exterior-rotor brushless IPM motor

Figure 1 shows a 3-phase, 12-pole/18-slot brushless IPM motor, where the rotor has embedded single-layer permanent magnets, and the permanent-magnet poles are in a V-shape. This brushless IPM motor is of an exterior-rotor configuration, which has been widely used as a hub motor (also called a directly driven wheel motor) for electrical scooters and vehicles, or as a spindle motor for numerical control machines. The stator, with fixed 3-phase coil windings, is arranged on the inner circumference of the rotor. Both the rotor and stator cores are formed by stacked metal laminated sheets. The rotor includes pairs of magnet insertion holes and pairs of magnetic barriers. Each pair of magnet insertion holes includes two magnet insertion

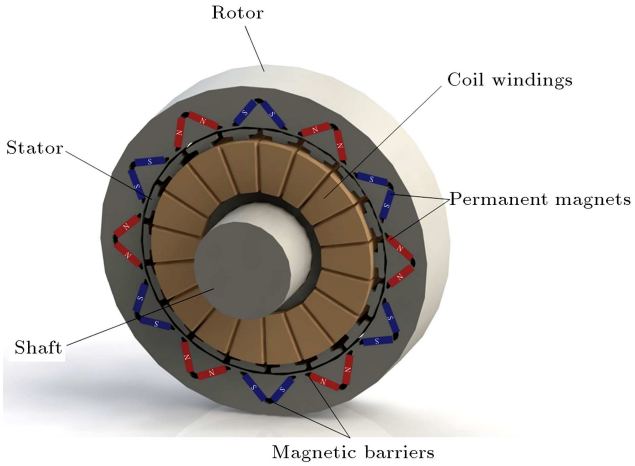

Figure 1. An exterior-rotor brushless IPM motor where the rotor has embedded single-layer permanent magnets and the permanent magnet poles are in a V-shape.

holes that are arranged in a V-shape. Two adjacent magnets buried in a pair of magnet insertion holes correspond to a single pole to provide the magnetizing flux. Therefore, such a magnet-retaining design prevents the magnets from flying apart, especially in high-speed applications. It also reduces the use of retaining rings for permanent magnets and simplifies the manufacturing process of the rotor for brushless IPM motors. The magnetic barrier inhibits short-circuiting of the magnetic flux between the pair of permanent magnets and also reduces the magnetic flux leakage. The output torque of brushless IPM motors consists of two major components. The first component is the electromagnetic torque developed by the flux linkage between the permanent magnet field of the rotor and the electromagnetic field of the stator. This is the same torque generated by brushless SPM motors. The second is the reluctance torque. The variable magnetic reluctance caused by the saliency structure of the rotor develops the reluctance torque of brushless IPM motors. Therefore, the resultant torque of the brushless IPM rotor is greater than the electromagnetic torque of the brushless SPM motor, and, hence, generates higher output torque.

3. Mitigation of cogging torque by FEA

The cogging torque of BLPM motors is the torque due to the mutual interaction between permanent-magnets mounted on the rotor and the teeth and slots structure formed on the stator, which is highly affected by the mechanical configurations and geometric dimensions of the rotor and stator. It is an open circuit torque, i.e. no stator current excitation is involved in the cogging torque production. The cogging torque is dependent on the rotor's angular position, and its periodicity relies on the number of magnetic poles on the rotor

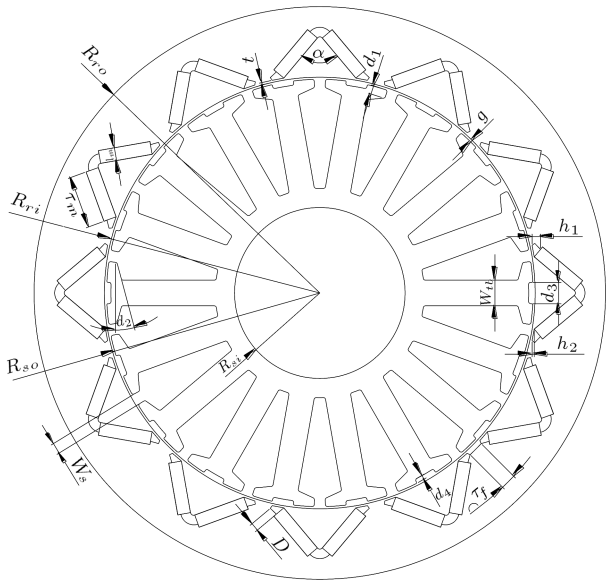

Figure 2. Cross section and geometric parameters of an exterior-rotor brushless IPM motor.

and the number of slots on the stator. Since it is an oscillatory and periodic torque that may induce unstable rotation of the rotor, mitigation of the cogging torque is a major task for electrical engineers. The brushless IPM motor, with permanent magnet poles in a V-shape, has many geometric parameters that may affect the cogging torque, so it is difficult to evaluate the cogging torque analytically. In this study, the FEA package, the Ansoft/Maxwell 2D field simulator, is used to accurately predict the cogging torque of the two-dimensional IPM motor configuration. Figure 2 shows the cross section and geometric parameters of the exterior-rotor brushless IPM motor, while Table 1 gives the related geometric and magnetic material data. The periodicity of the cogging torque of this brushless IPM motor is:

$$360^\circ/lcm(P,S) = 360^\circ/lcm(12,18) = 360^\circ/36 = 10^\circ. \quad (1)$$

In Eq. (1), symbol P is the number of magnet poles, symbol S is the number of stator slots and $lcm(P,S)$ is the least common multiplier between P and S. The computed cogging torque of the brushless IPM motor between 0° and 10° is shown in Figure 3. The peak value of the cogging torque is 4.77 Nm which occurs at about 1.5 mechanical degrees and not half of 5 mechanical degrees. It should be mentioned that the discrepancy of the peak position is mainly caused by the salient effects of the salient poles on the rotor for the brushless IPM motor. An alternation of one geometric parameter of the rotor or stator may result in a variation of the cogging torque. In what follows, geometric design parameters, including the magnet

Table 1. Geometric and magnetic material data of an exterior-rotor brushless IPM motor.

NdFeB magnet properties (BNP 12)		
Items	**Symbol**	**Values**
Remanence (T)	B_r	0.76
Coercivity (A/m)	H_c	-480000
Relative permeability	μ_r	1.26
Direction of magnetization	–	Parallel
Magnet thickness (mm)	l_m	6
Magnet width (mm)	τ_m	24.50
Width between two adjacent air barriers (mm)	τ_f	10.95
Geometric parameters		
Items	**Symbol**	**Values**
Number of phases	N_{ph}	3
Number of magnet poles	P	12
Number of armature slots	S	18
Air gap length (mm)	g	1
Slot opening arc (degree)	W_s	3
Rotor's outer radius (mm)	R_{ro}	134
Rotor's inner radius (mm)	R_{ri}	101
Stator's outer radius (mm)	R_{so}	100
Stator's inner radius (mm)	R_{si}	40
Bridge width (mm)	t	1
Air barrier length 1 (mm)	h_1	3.75
Air barrier length 2 (mm)	h_2	1.38
Air barrier width (mm)	D	2
Magnet span angle (degree)	α	90
Shoe depth (mm)	d_1	2
Shoe ramp (degree)	d_2	0
Dummy slot width (mm)	d_3	0
Dummy slot depth (mm)	d_4	0
Tooth width (mm)	w_{tb}	12
Stack length (mm)	L	55

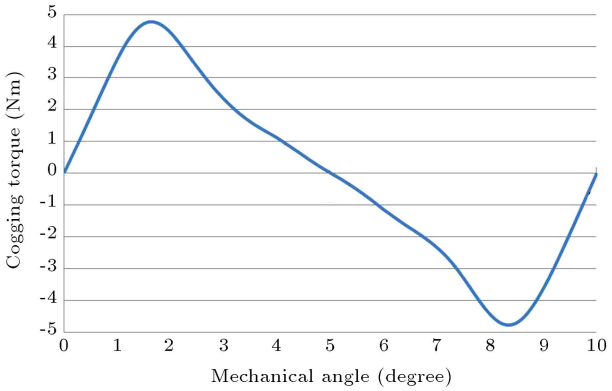

Figure 3. Cogging torque waveform of the brushless IPM motor shown in Figure 2 and Table 1.

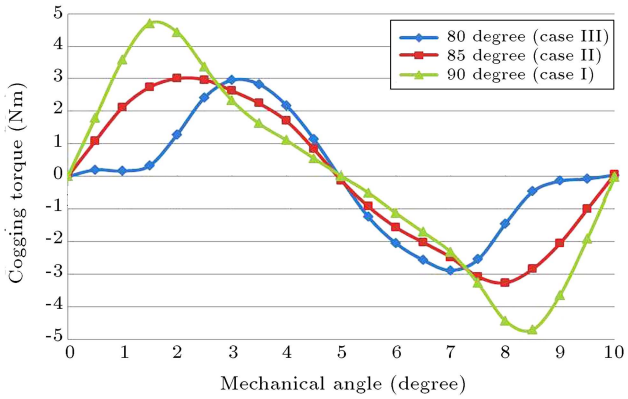

Figure 4. Comparison of cogging torque for brushless IPM motors with different magnet span angles, α.

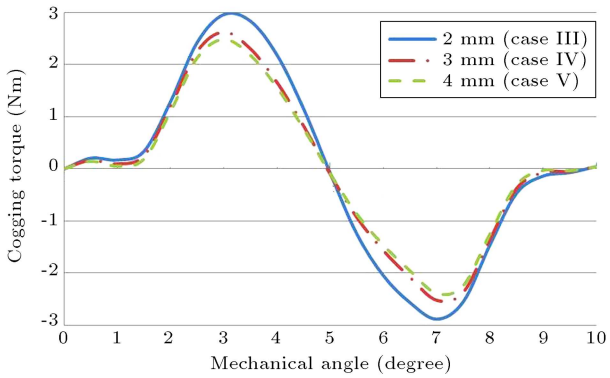

Figure 5. Cogging torque waveforms versus the angular position of the rotor for brushless IPM motors with different shoe depths, d_1.

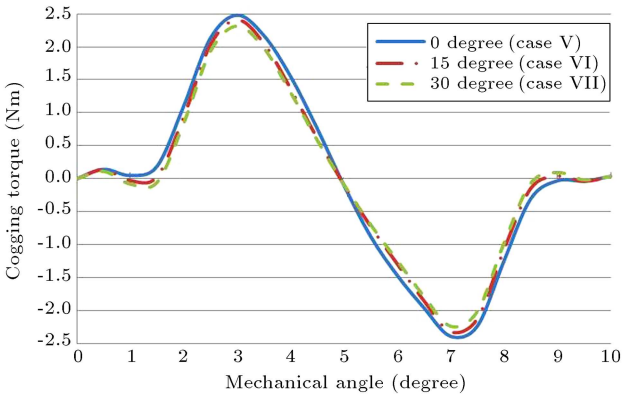

Figure 6. Cogging torque waveforms of brushless IPM motors with different shoe ramps, d_2.

span angle, α, of the rotor, shoe depth, d_1, shoe ramp, d_2, of the stator, dummy slots notched on the stator, dummy slot depth, d_4, as well as dummy slots notched on both the stator and rotor, are discussed to mitigate the undesirable cogging torque. Since the volume of permanent magnets dominates the cogging torque, the volume of permanent magnets of each design case is designed to be identical for comparison purposes.

3.1. Magnet span angle, α

Figure 4 shows cogging torque waveforms for the brushless IPM motor presented with different magnetic span angles, α. It indicates that with a decrease in the magnet span angle, the peak value of the cogging torque decreases. The peak value of the cogging torque of the IPM motor with a magnet span angle equal to 80° (design case III), decreases by 37% in comparison with that of the original IPM motor with a magnet span angle equal to 90° (design case I).

3.2. Length of shoe depth d_1 and angle of shoe ramp d_2

The periodic cogging torque can be represented to the integration of the tangential and normal magnetic flux components within the air gap [15]. Because the normal and tangential magnetic flux components within the air gap vary with the geometric shape of the pole shoes of the stator, the mitigation of the cogging torque can be achieved by modifying the shape of the pole shoe, including the length of shoe depth, d_1, and the angle of shoe ramp, d_2, as shown in Figure 2. Figure 5 shows the cogging torque waveforms of brushless IPM motors with different shoe depths, d_1. It can be seen that the peak values of the cogging torque decrease with the increase in shoe depth. Influences of the angle of shoe ramp, d_2, on the cogging torque are shown in Figure 6. It is interesting that the peak values of the cogging torque decrease with the increase in the shoe ramp. Table 2 lists the peak values of the cogging torque for each design case, with different magnetic span angles, α, shoe depths, d_1, and shoe ramps, d_2. By determining the magnet span angle $\alpha = 80°$, the length of shoe depth, $d_1 = 4$ mm, and the angle of shoe ramp $d_2 = 30°$, i.e. design case VII, the peak value of the cogging torque is reduced to 2.32 Nm, which decreases 50.6% in comparison with that of the original brushless IPM motor (design case I).

3.3. Dummy slots notched on the stator

Adding dummy slots on the stator is one popular technique for reducing the cogging torque for brushless SPM motors. To investigate the feasibility of cogging torque reduction of dummy slots notched on the stator of brushless IPM motors, a dummy slot with a rectangular shape is further notched on each pole shoe of the stator for design case VII, which is design case VIII shown in Table 3. The dummy slot width, d_3, and dummy slot depth, d_4, are 10 mm and 2 mm, respectively. Figure 7 depicts that 67.7% cogging torque amplitude reduction is achieved in design case VIII in comparison with that of the original brushless IPM motor (design case I). The reason for this is that the dummy slot on the stator increases the fundamental frequency of the cogging torque and, hence, reduces its amplitude simultaneously. In addition, dummy slots notched on the rotor increase the average length

Table 2. Comparisons of maximum cogging torques for different design cases.

Design case	Geometric parameters			Maximum cogging torque (Nm)	Difference (%)
	α (°)	d_1 (mm)	d_2 (°)		
I (Original design)	90	2	0	4.70	Datum
II	85	2	0	3.01	-36.0%
III	80	2	0	2.96	-37.0%
IV	80	3	0	2.62	-44.3%
V	80	4	0	2.48	-47.2%
VI	80	4	15	2.41	-48.7%
VII	80	4	30	2.32	-50.6%

Table 3. Comparisons of maximum cogging torque for different dummy slot depths.

Design case	Geometric parameters					Maximum cogging torque (Nm)	Difference (%)
	α (°)	d_1 (mm)	d_2 (°)	d_3 (mm)	d_4 (mm)		
I (Original design)	90	2	0	0	0	4.70	Datum
VIII	80	4	30	10	2.0	1.52	-67.7%
IX	80	4	30	10	1.5	1.19	-74.7%
X	80	4	30	10	1.0	0.98	-79.1%

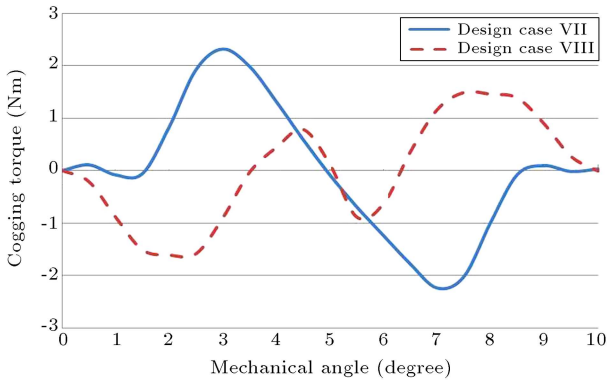

Figure 7. Cogging torque waveforms versus the angular position of the rotor for design case VII and design case VIII with dummy slots on the stator.

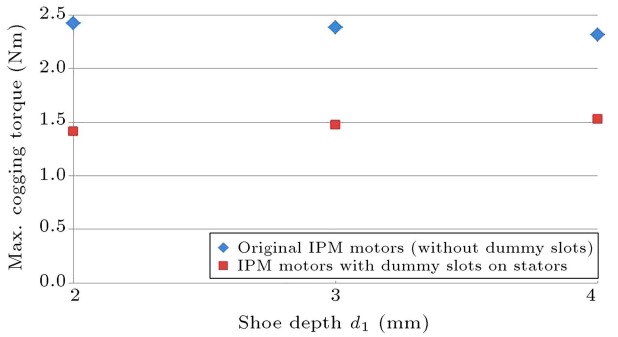

Figure 8. Peak values for cogging torques versus the shoe depth d_1 for brushless IPM motors with notched dummy slots on stators and those motors without notched dummy slots ($\alpha = 80°$, $d_2 = 30°$, $d_3 = 10$ mm and $d_4 = 2$ mm).

and reluctance of the air gap, so as to reduce the amplitude of the cogging torque. Figure 8 indicates that all brushless IPM motors with notched dummy slots on stators possess smaller cogging torques than those motors without notched dummy slots.

3.4. Length of dummy slot depth d_4

Theoretically, the cogging torque is equal to the variation of magnetic energy stored in the air gap of the electric motor [16]. Because the variation in the dummy slot depth alters the air-gap stored energy, it may affect the amplitude of the cogging torque. Figure 9 presents cogging torque waveforms versus the angular position of the rotor for brushless IPM motors with different dummy slot depths, d_4. It is

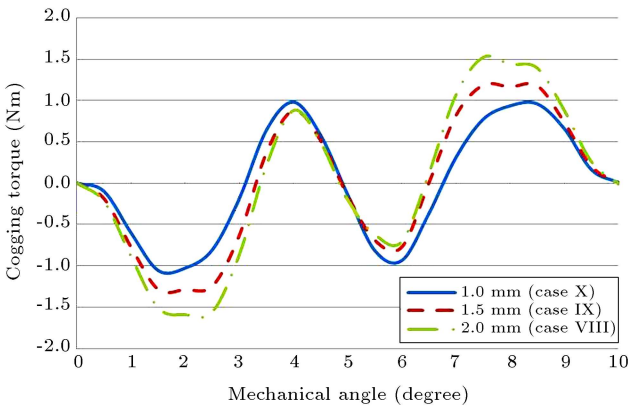

Figure 9. Comparison of cogging torque for brushless IPM motors with different dummy slot depths, d_4.

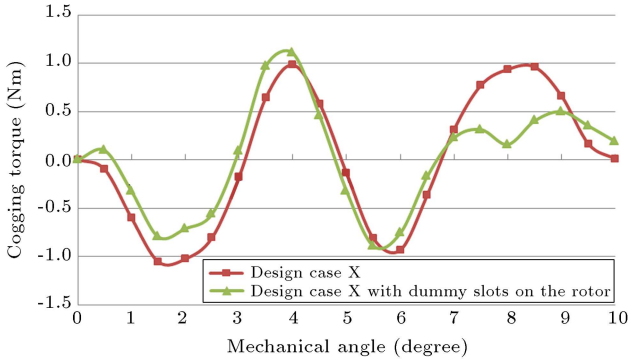

Figure 10. Cogging torque waveforms versus the angular position of the rotor for design case X and the same design case adding dummy slots on the rotor.

worth mentioning that the peak values of the cogging torque decrease with the decrease in dummy slot depth. Table 3 shows that the peak value of the cogging torque for design case X decreases 79.1% in comparison with that of the original brushless IPM motor (design case I).

3.5. Dummy slots notched on both the stator and rotor

Figure 10 illustrates the cogging torque waveforms for design case X, and the same design case adding dummy slots on the rotor. It shows that the strategy for adding dummy slots on the rotor is not effective on reducing the peak value of the cogging for this design case. This is because dummy slots notched on the inner circumference of the rotor do not effectively alter the magnetic energy and magnetic flux distribution within the air-gap of design case X.

4. Conclusion

This paper investigates the influence of geometric design parameters on the cogging torque of an exterior-rotor brushless IPM motor. The strategy for minimizing the amplitude of the cogging torque for the presented brushless IPM motor, with magnets arranged in a V-shape, is to increase the shoe depth and shoe ramp of the pole shoe of the stator, to decrease the magnet span angle of the rotor, to add dummy slots on the pole shoes of the stator and to decrease the dummy slot depth on the stator, which assists in restraining the vibration and acoustic noise of brushless IPM motors. The results show that design case X possesses the smallest cogging torque, which is decreased 79.1% in comparison with that of the original brushless IPM motor. Although the approaches mentioned in this study are effective in mitigating the cogging torque of brushless IPM motors, they may also depress the electromagnetic torques of electrical motors that are undesirable for motor designers. This is because the modifications of the rotor and stator geometries may affect the amount of fluxes that cross the air gap to link the coils of the phase windings on the stator. However, it is difficult to predict the difference of the magnetic fluxes that cross the air gap analytically as the rotor and stator geometries are modified. Future work on this study will discuss the influence of geometric parameters on the output torque of brushless IPM motors.

Acknowledgment

The authors thank the National Science Council (Taiwan, R.O.C) for supporting this research under Grant No.102-2221-E-224-016-MY2. They also thank the National Yunlin University of Science and Technology for providing support research apparatus and Ansoft/Maxwell software.

References

1. Kenjo, T. and Nagamori, S., *Brushless Motors: Advanced Theory and Modern Applications*, 3rd Edn., Sogo Electronics Press, Tokyo, Japan, pp. 1-2 (2003).
2. Gebregergis, A., Chowdhury, M., Islam, M. and Sebastian, T. "Modeling of permanent magnet synchronous machine including torque ripple effects", *2013 IEEE Energy Convers. Congr. and Expos.*, Denver, USA, pp. 2108-2114 (2013).
3. Fei, W. and Zhu, Z.Q. "Comparison of cogging torque reduction in permanent magnet brushless machines by conventional and herringbone skewing techniques", *IEEE Trans. Energy Convers.*, **28**(3), pp. 664-674 (2013).
4. Hsieh, W.H. and Tseng, C.Y. "Acceleration improvement for coil winders of RRRCC type by variable input speed method", *J. Vibroeng.*, **14**(4), pp. 1459-1468 (2012).
5. Jin, C.S., Jung, D.S., Kim, K.C., Chun, Y.D., Lee, H.W. and Lee, J. "A study on improvement magnetic torque characteristics of IPMSM for direct drive washing machine", *IEEE Trans. Magn.*, **45**(6), pp. 2811-2814 (2009).
6. Shi, J., Chia, F., Li, X. and Cheng, S. "Study of the number of slots/pole combinations for low speed high torque permanent magnet synchronous motors", *2011 Int. Conf. on Electr. Mach. and Syst.*, Beijing, China, pp. 1-3 (2011).
7. Zhu, Z.Q. and Howe, D. "Influence of design parameters on cogging torque in permanent magnet machines", *IEEE Trans. Energy Convers*, **15**(4), pp. 407-412 (2000).
8. Islam, R., Husain, I., Fardoun, A. and McLaughlin, K. "Permanent-magnet synchronous motor magnet designs with skewing for torque ripple and cogging torque reduction", *IEEE Trans. Ind. Appl.*, **45**(1), pp. 152-160 (2009).

9. Chu, W.Q. and Zhu, Z.Q. "Investigation of torque ripples in permanent magnet synchronous machines with skewing", *IEEE Trans. Magn.*, **49**(3), pp. 1211-1220 (2013).

10. Xua, C., Chen, Z., Shi, T. and Wang, H. "Cogging torque modeling and analyzing for surface-mounted permanent magnet machines with auxiliary slots", *IEEE Trans. Magn.*, **49**(9), pp. 5112-5123 (2013).

11. Miller, T.J.E. and Hendershot, Jr. J.R., *Design of Brushless Permanent Magnet Motors*, 1st Edn., Clarendon Press, Ohio, USA, pp. 4-28 (1994).

12. Azar, Z., Zhu, Z.Q. and Ombach, G. "Influence of alternate slot openings on torque-speed characteristics and cogging torque of fractional slot IPM brushless AC machines", *2013 IEEE Energy Convers. Congr. and Expos.*, Phoenix, USA, pp. 2244-2251 (2011).

13. Wu, Y.C. and Hong, Y.C. "Cogging torque and torque ripple reduction of a novel exterior-rotor geared motor", *J. Vibroeng.*, **14**(4), pp. 1477-1485 (2012).

14. Wu, Y.C. and Yan, H.S. "Design of surface-mounted permanent-magnet brushless DC motors combined with gear mechanisms", *Trans. Can. Soc. Mech. Eng.*, **37**(3), pp. 439-448 (2013).

15. Lin, Y.K., Hu, Y.N., Lin, T.K., Lin, H.N., Chang, Y.H., Chen, C.Y., Wang, S.J. and Ying, T.F. "A method to reduce the cogging torque of spindle motors", *J. Magn. Magn. Mater.*, **209**(1-3), pp. 180-182 (2000).

16. Hwang, S.M., Eom, J.B., Hwang, G.B., Jeong, W.B. and Jung, Y.H. "Cogging torque and acoustic noise reduction in permanent magnet motors by teeth pairing", *IEEE Trans. Magn.*, **36**(5), pp. 3144-3146 (2000).

Biographies

Yi-Chang Wu received BS and MS degrees from the National Sun Yat-Sen University (NSYSU), Kaohsiung, Taiwan, R.O.C., in 1995 and 1997, respectively, and a PhD degree from the National Cheng Kung University (NCKU), Tainan, Taiwan, R.O.C, in 2005, all in Mechanical Engineering.

He is currently Associate Professor in the Department of Mechanical Engineering at National Yunlin University of Science & Technology (NYUST), Yunlin, Taiwan, R.O.C. His research interests include creative machine design, brushless permanent-magnet motor design, and novel magnetic mechanism design.

Yueh-Tung Chen received an MS degree in Mechanical Engineering from the National Yunlin University of Science & Technology (NYUST), Yunlin, Taiwan, ROC. His research interests are in the areas of permanent-magnet motor design, magnetic gear mechanism design, and finite-element analysis.